analytical chemistry

Technical Note

Cite This: Anal. Chem. XXXX, XXX, XXX−XXX

pubs.acs.org/ac

Dynamic Generation of Concentration- and Temporal-Dependent Chemical Signals in an Integrated Microfluidic Device for Single-Cell Analysis

Alan M. Gonzalez-Suarez,[†] Johanna G. Peña-del Castillo,[‡] Arturo Hernández-Cruz,[‡] and Jose L. Garcia-Cordero*,[†]

[†]Unidad Monterrey, Centro de Investigación y de Estudios Avanzados del Instituto Politécnico Nacional, Parque PIIT, Apodaca, Nuevo León, 66628, México

[‡]Departamento de Neurociencia Cognitiva y Laboratorio Nacional de Canalopatías, Instituto de Fisiología Celular, Circuito de la Investigación Científica s/n Ciudad Universitaria, Universidad Nacional Autónoma de México, Ciudad de México 04510, México

Supporting Information

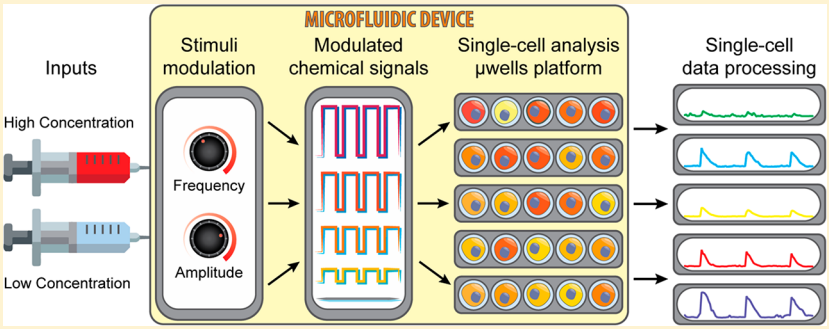

ABSTRACT: Intracellular signaling pathways are affected by the temporal nature of external chemical signaling molecules such as neurotransmitters or hormones. Developing high-throughput technologies to mimic these time-varying chemical signals and to analyze the response of single cells would deepen our understanding of signaling networks. In this work, we introduce a microfluidic platform to stimulate hundreds of single cells with chemical waveforms of tunable frequency and amplitude. Our device produces a linear gradient of 9 concentrations that are delivered to an equal number of chambers, each containing 492 microwells, where individual cells are captured. The device can alternate between the different stimuli concentrations and a control buffer, with a maximum operating frequency of 33 mHz that can be adjusted from a computer. Fluorescent time-lapse microscopy enables to obtain hundreds of thousands of data points from one experiment. We characterized the gradient performance and stability by staining hundreds of cells with calcein AM. We also assessed the capacity of our device to introduce periodic chemical stimuli of different amplitudes and frequencies. To demonstrate our device performance, we studied the dynamics of intracellular Ca^{2+} release from intracellular stores of HEK cells when stimulated with carbachol at 4.5 and 20 mHz. Our work opens the possibility of characterizing the dynamic responses in real time of signaling molecules to time-varying chemical stimuli with single cell resolution.

A current trend in biology is deciphering how cells process and relay information through the dynamics of signaling molecules,[1,2] as opposed to steady state conditions.[3] A chemical temporal signal encodes information mainly in the form of its identity (activity or state), amplitude (concentration), frequency, duration, localization, phase, cumulative signal, and delay.[1,2] The periodicity of these signals can range from microseconds to days[4,5] and can be classified as either frequency (FM) or amplitude (AM) modulated.[2] A cell decodes these signals through intracellular signaling effectors whose actions affect gene expression and modify cellular activities.[6] Likewise, it is now recognized that even when challenged with the same stimulus, genetically identical cells can respond with different dynamical patterns.[1] Monitoring single cells over time is essential to discover the causes of this heterogeneity, which in turn can help to understand the causes for the variability of these signaling mechanisms.[7]

Thus, to decipher signaling mechanisms, there is a need of experimental techniques that can emulate physiological chemical signals with different concentrations and short time scale (from seconds to minutes) while simultaneously monitoring hundreds of single cells in real time. However, conventional laboratory tools are typically limited to the generation of stimulus with abrupt changes of concentrations, few cells at a time, and with limited temporal resolution.[8−10]

Received: May 31, 2018
Accepted: June 19, 2018
Published: June 19, 2018

DOI: 10.1021/acs.analchem.8b02442
Anal. Chem. XXXX, XXX, XXX−XXX

Microfluidic devices for generating dynamic chemical signals have evolved from producing simple waveforms to more sophisticated ones capable to tune concentration and time periodicity on demand,[11−15] with some of them able to introduce chemical noise on these signals.[16] These devices have been used to study the response of single cells to time-varying stimulus.[8,16−18] However, one major technical hurdle has been to engineer a device to simultaneously deliver chemical signals of varying frequency and amplitude (concentration) to a large number of individual cells under low shear-stress conditions. These experimental conditions, in combination with image-acquisition and image analysis technologies, will provide a more quantitative picture of phenotypic cell-to-cell variability and help uncover novel regulation mechanisms.[19] Also, such a device could greatly expedite the characterization of cellular responses in pharmacological and physiological studies.

In a step toward this direction, we introduce an integrated microfluidic device to expose repetitively single cells to chemical signals of different concentration over long periods of time. Compared to other recently developed devices (see Table S1), our technology allows hundreds of cells to be studied in a low shear-stress environment. Employing fluorescent time-lapse microscopy, we can monitor minute changes in fluorescence intensity of individual cells. As demonstrated here, in one instance we were able to acquire 750,720 data points from one experiment. The device design, operation, and characterization is described as well as its application to study the intracellular calcium ($[Ca^{2+}]i$) signals of HEK-293 cells (a nonadherent cell line widely used for transfection and signaling studies[20]) under the stimulation by time-varying chemical signals.

MATERIALS AND METHODS

Microfabrication. The microfluidic device was fabricated by standard multilayer soft lithography. See details in the Supporting Information.

Materials. Reagents and materials used for the fabrication and the assays can be found in the Supporting Information.

Cell Culture. Human Embryonic Kidney cells 293 (HEK-293) were grown in DMEM/F-12 supplemented with penicillin-streptomycin (10 000 U/mg^{-1} mL^{-1}) and 10% fetal bovine serum at 37 °C in 5% CO_2. Cells were harvested with TrypLE express, centrifuged at 1200 rpm for 5 min, and resuspended in 3 mL of Krebs-HEPES (pH 7.4) solution at ∼5 × 10^6 cells/mL. For Calcein-AM experiments, cells were centrifuged and washed with PBS 1× before being seeded in the microfluidic device. For calcium dynamics, cells were incubated with 2 μM of Fluo-8-AM for 30 min at room temperature, centrifuged, washed with Krebs-HEPES solution, and resuspended to obtain a concentration of 5 × 10^6 cell/mL.

Characterization of the Gradient Generation and Pulses. Solutions of Dextran-rhodamine (40 kDa) at 100 μg/mL and FITC at 10 μg/mL were injected into the device through the CGG inlets using a syringe pump (780200, KD Scientific), at flow rates ranging from 0.5 to 2 μL/min. Images were acquired with an inverted epifluorescence microscope (DMI6000 B, Leica Microsystems) equipped with a motorized stage and autofocus. Each chamber was imaged continuously for 5 min, for a total of 45 min for each frequency.

Calcein Staining and $[Ca^{2+}]i$ Dynamics. Single-cells were trapped inside microwells and isolated from fluid flow by closing all the valves surrounding the chambers. Experiments were made with the agonist of interest. A solution of Calcein-AM at 3 μM was prepared on PBS 1×. Krebs HEPES buffer was used to perfuse the device at all times. Solutions of Carbachol and caffeine at 10 μM and 30 mM, respectively, were prepared in Krebs HEPES.

Data Analysis. Cells trapped in the microwells were observed with a 10×/0.25 NA Hi PLAN objective and a set of fluorescent filter sets (L5 and N3). The exposure time of the camera was set to 250 ms for $[Ca^{2+}]i$ dynamics observation and 180 ms for calcein experiments. A set of images from all the chambers were acquired at 8.7 s intervals for $[Ca^{2+}]i$ dynamics, and 13 s intervals for calcein staining experiments. Images were processed using a custom script (Matlab 2015b, Mathworks) to obtain the fluorescence intensity from each cell over time. Heatmaps representing the fluorescent intensity values of each cell are generated using a K-means clustering algorithm that organizes data according to fluorescence intensity values.

RESULTS AND DISCUSSION

Microfluidic Device Design and Operation. We designed a microfluidic device consisting of two main modules: a concentration gradient generator (CGG), and a perfusion module with nine microchambers, each containing 492 microwells (well height and diameter, 20 μm) for single-cell trapping, Figure 1 and Figure S1. The CGG consists of a network of microchannels with controlled resistance that produces a gradient of 9 concentrations with a linear profile.[21] To produce temporal- and concentration-varying stimuli, the gradient generator is controlled using microvalves. Each of the nine outlets from the CGG leads to a single microchamber, where cells are exposed in parallel to different concentrations of the same molecule. To capture cells, we employ microwells, a technology that allows cells to experience low shear-stresses while being perfused at different flow rates.[22] After the chemical stimuli passes through all the microchambers they converge into a single outlet for waste removal. The device is controlled by 78 microvalves operated from 10 control fluidic channels.

The operation of the device starts by closing all the valves surrounding the microchambers. The gradient is then generated and after it has reached a steady state (∼20 s), the bottom and top valves of the microchambers together with the drain channel valves are closed. Then, a suspension of cells is injected through one of the inlets and flowed through the 9 chambers. To trap the cells, we implemented "cycles of sedimentation":[22] with the flow stopped the cells so that cells are allowed to settle for 15 s (Figure 1c). The shear stress generated on a single cell placed inside a μwell is 0.128 dyn/cm^2 (Figure S2). This small value, comparable to previously reported devices (0.1−5 dyn/cm^2), emphasizes the innocuous nature of these microwells for this study. After the cells have been trapped, all the valves surrounding the microchambers are closed (Figure 1d,e).

Gradient Formation. The length of all the branched channels in the CGG was designed to allow a molecule of 40 kDa (larger than most drugs, hormones, and agonists) to mix completely by diffusion before advancing to the next branch, even for flow rates as high as 6 μL min^{-1}. To test the CGG we injected a solution of Dextran-Rhodamine (D-R, MW = 40 kDa) in one inlet while fluorescein isothiocyanate (FITC, MW = 389 Da) was injected in the second inlet. We observed the formation of two opposing linear gradients, despite the two

DOI: 10.1021/acs.analchem.8b02442
Anal. Chem. XXXX, XXX, XXX−XXX

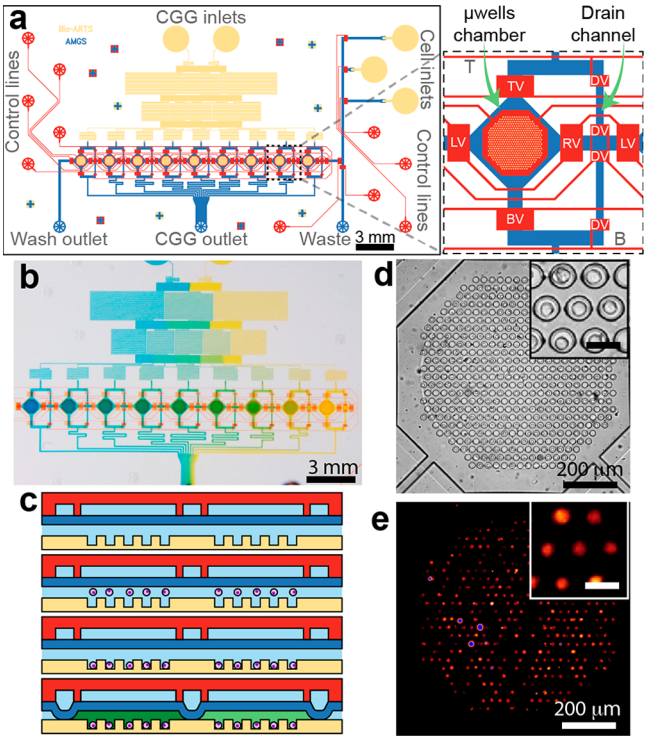

Figure 1. Microfluidic device design and principle. (a) Microfluidic device design: blue corresponds to the flow layer, red to the control layer, and yellow to the microwells and gradient generator layer. Close-up to one of the microwell chambers surrounded by a drain channel is shown on the right. DV denotes drain channel valves. The prefix T, B, L, and R indicate top, bottom, left, and right valves, respectively. (b) Photograph of the device; observe how colored fluids form a gradient. (c) Schematic of a cross-sectional view of a microchamber, showing from top to bottom: cells being flowed, settling down into the microwells, valves being activated, and microchambers being exposed to the stimulus (green color). (d,e) Bright-field and fluorescence micrographs of a single microchamber with HEK-293 cells trapped inside microwells and stained with Fluo-8. Insets, enlargement of a section of the microchamber. Scale bars = 30 μm.

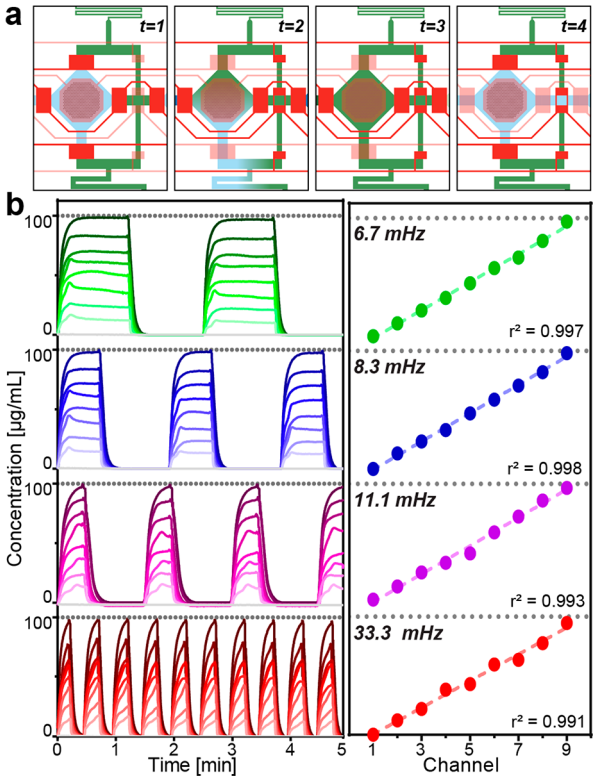

Figure 2. Pulse-formation characterization. (a) Schematic of the operation of the device for generating a periodic chemical stimulus in a single chamber. Red solid or translucent color represents closed or open valves, respectively. At t = 1, the valves enclosing the chamber are closed while the drain channel valves are open, allowing fluid from the CGG to bypass the chamber through the drain channel. Next, at t = 2, the drain channel valves are closed and the chamber top and bottom valves open, allowing solution to flow into the chambers until they are entirely filled, t = 3. For the washing step, top and bottom valves are closed, t = 4. The sequence is repeated for the desired number of pulses (scale bar = 500 μm). (b) Graph showing the generation of periodic chemical signals (Dextran 40 kDa) in each of the nine microchambers at four different frequencies for 5 min. The darkest color corresponds to fluorescence intensity of the chamber receiving the highest dye concentration. The graphs to the right show the maximum concentrations reached in each chamber, n = 20; error bars, 1 SD.

orders difference in molecular weight (Figures S3 and S4). Note that to ensure the correct formation of the gradient in an assay, any of these molecules can function as a tracer when mixed with the stimuli solution.

Pulse Stimulation. We created periodic stimuli consisting of identical pulses of a given concentration separated by an interval of perfusion with a control, washing solution. To pulse different concentrations through all the microchambers we included a drain channel that runs parallel to each microchamber, Figure 1a. The operation involves initially forming the gradient through the drain channel by closing the valves surrounding the microchambers but keeping the valves of the drain channel open, Figure 2a, t = 1. Once the gradient is fully formed, drain-channel valves are closed while the two vertical valves of the microchamber are opened, t = 2. The corresponding solution then flows through each microchamber for a time set by the user, t = 3. To wash the microwells all the valves are closed except for the valves separating the microchambers and liquid is introduced from left to right or vice versa, t = 4. This process can be repeated several times using a computer software that automatically activates the microfluidic valves and sets the number and duration of pulses and washing periods.

We assessed the performance of our device to produce periodic chemical waveforms of different frequencies and concentrations. A solution of D-R and PBS was flowed through the CGG channels followed by a washing step in all the chambers with clean PBS. The half-period of the chemical waveform is defined by the slowest filling time of the microwells. Measuring the change in fluorescence intensity over time in different sections of the microchamber, we determined the minimum time required to completely exchange solutions (D-R for PBS and vice versa) at a flow rate of 2 μL min^{-1}. The microwells located downstream within the chamber took the longest to fill, ~15 s vs ~7 s upstream (Figure S5). He et al.[8] were able to produce chemical signals with a 20 s period, and their device produced shear stresses similar to those produced in our device, but their signal quickly degraded as it traveled down the channel, thus only effectively exposing dozens of cells to the stimulus. In our device, this

DOI: 10.1021/acs.analchem.8b02442
Anal. Chem. XXXX, XXX, XXX−XXX

period could be further reduced by decreasing the size of the microchambers and the number of microwells in it, albeit at the cost of stimulating less cells.

Next, we tested the ability of the device to create periodic stimuli through all the chambers and at different concentrations. Pulses of D-R were generated at four different frequencies (periods): 33.3 mHz (30 s), 11.1 mHz (90 s), 8.3 mHz (120 s), and 6.7 mHz (150 s). Figure 2b shows the periodic stimuli produced by the device. All the periodic stimuli reached the expected concentration in 15 s, producing several consecutive, reproducible cycles. The waveform of the concentration pulse in some microchambers show some imperfections like a small overshoot (<10%) observed at every third chamber when reaching their peak concentration. Nevertheless, this small defect is not likely to have a significant impact on cellular biological assays.

Calcein-AM Concentration Gradient Experiments. To demonstrate the performance of the CGG, we exposed hundreds of cells with calcein AM, a membrane-permeable fluorescent marker of cell viability. Endogenous esterases in the cell cytoplasm cleave the acetoxymethyl (AM) ester of the calcein-AM molecule releasing free calcein, which is non-permeant and therefore remains trapped inside the cell. The intracellular fluorescence intensity is proportional to the concentration of calcein trapped and thus to the activity of cell esterases. Using our microfluidic device, HEK-293 cells were captured inside microwells and exposed for 2 h to different concentrations of calcein-AM, ranging from 0 to 3 μM. The staining of cells over time is shown in Figure 3. Using custom image analysis algorithms (Figure S6), we tracked a total of 1,560 cells every 14 s for a total of 750,720 data points for the duration of the assay. End-point fluorescence histograms were fitted with a Gaussian distribution, reflecting the variation of esterase activity in the cells. Overall, mean fluorescence intensity increases over time, and the end-point data is proportional to the calcein-AM concentration (Figure S7). Fluorescence does not increase in the chamber where calcein-AM is not present. An increasing number of population studies with single-cell resolution confirm that genetically identical cells in a uniform environment can display different phenotypes, which are often masked by measurements of mean values from cell populations.[23] As demonstrated here, our device discloses information from hundreds of individual cells in parallel under distinct conditions, without dislodging the cells from the microwells.

Ca^{2+} Concentration Dynamics. Intracellular Ca^{2+} concentration ($[Ca^{2+}]i$) dynamics is a time-dependent signal that regulate several cellular mechanisms, from gene transcription to cell death,[24,25] at different time-scales. Wild type HEK-293 cells are known to endogenously express the M_1 muscarinic receptor.[26] The activation of M_1 receptors with carbachol produces inositol-1,4,5-triphosphate ($InsP_3$) at the plasma membrane which diffuses and binds to $InsP_3$ receptors and triggers the release of Ca^{2+} from intracellular stores, thus increasing $[Ca^{2+}]i$. Furthermore, changes in $[Ca^{2+}]i$ in response to increasing agonists concentration can be gradual but often involves more complex signaling like oscillatory responses "spikes" whose properties (amplitude, frequency, localization) depend on the properties of the stimulus.[27,28]

To study population $[Ca^{2+}]i$ dynamics in our device, HEK-293 cells were incubated with Fluo-8-AM, before being introduced into the microfluidic device. When Fluo-8 binds free Ca^{2+}, cell fluorescence intensity increases, reflecting

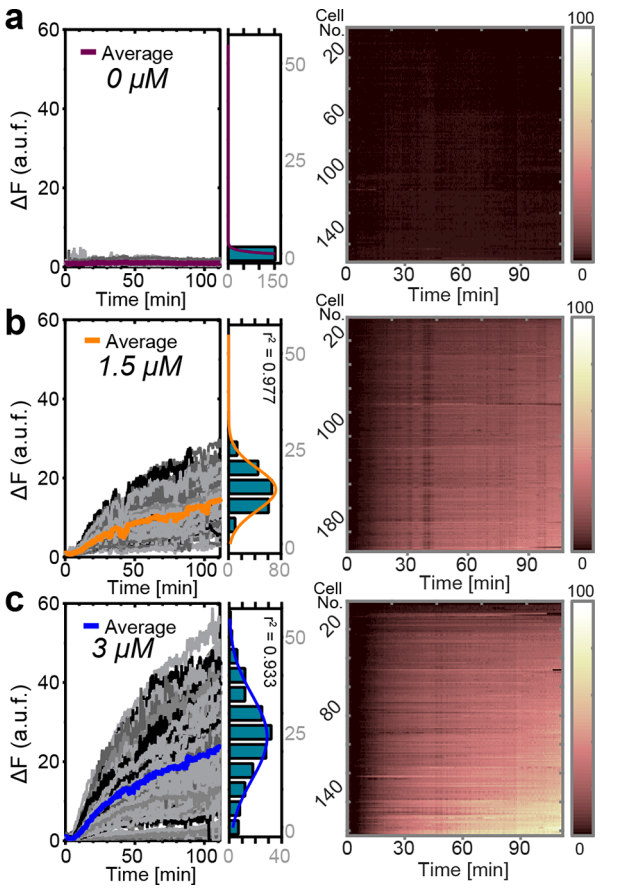

Figure 3. Calcein staining of HEK-293 cells. Left graphs show traces of individual cells stimulated with Calcein-AM: (a) 0, (b) 1.5, and (c) 3 μM. The colored line represents the average of all the traces. End-point histograms or the fluorescence in the cell population was fitted to a Gaussian distribution. The heat maps (right) show the fluorescence intensity of individual cells through time, normalized to the intensity of the highest concentration of Calcein-AM. Additional traces for the remaining concentrations are illustrated in Figure S8.

$[Ca^{2+}]i$ rises. Cells were stimulated with carbachol (MW = 182 Da) through the CGG at concentrations ranging from 0 μM to 10 μM. Five stimulation pulses were given to a group of cells and 10 pulses to another group (in different devices), with two frequencies of 4.5 (Figure 4 and Figure S9) and 20 mHz (Figures S10 and S11), respectively. Using time-lapse fluorescence microscopy, fluorescence intensity from individual cells was measured only in five of the nine chambers.

The graphs in Figure 4 a,b and Figure S9 show the mean response of all cells in a microchamber (solid line) and of the responding cells only (dashed lines). A heatmap showing the response of individual cells is shown in Figure 4c (one cell per row). At 4.5 mHz, ~15% of the cells released intracellular Ca^{2+} from the fourth pulse onward in response to a concentration of 1.25 μM. This percentage increases to ~25% at a concentration of 3.75 μM with most cells responding from the second pulse. At higher concentrations, the cells start responding from the first pulse with the same frequency they are stimulated with. This is accompanied by an increased percentage of cell recruitment: ~30% at 6.26 μM and ~50% at 10 μM (Figure 4c). At a frequency of 20 mHz (Figures S10 and S11) we noticed that cells tended to respond from the first stimulation pulse from the lowest agonist concentration: 1.25

DOI: 10.1021/acs.analchem.8b02442
Anal. Chem. XXXX, XXX, XXX−XXX

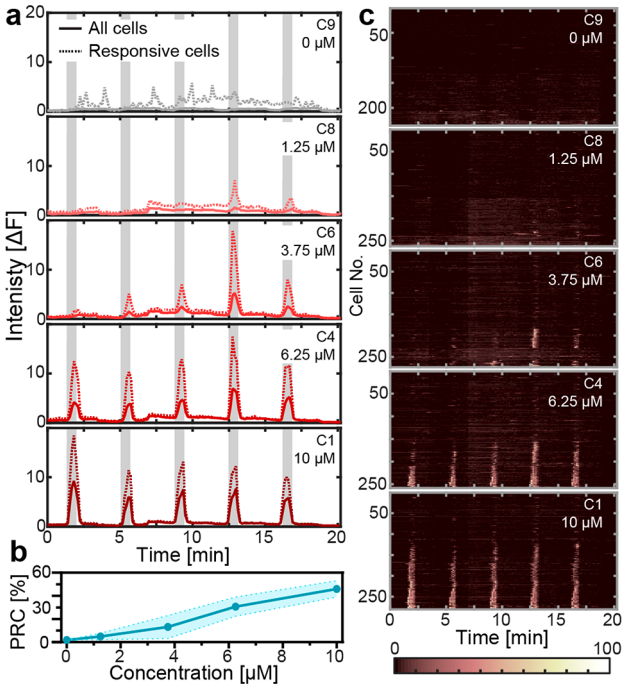

Figure 4. Periodic stimulation of HEK-293 cells with carbachol. (a) The graph shows average responses for a group of cells stimulated at 4.5 mHz. Solid lines show average response of all cells; dashed lines show average response of only responsive cells. Carbachol exposure is represented by vertical gray bars. (b) Graphs showing the percentage of responsive cells (PRC) for data shown in part a at each concentration. The dimmed area around the average line shows the standard deviation. (c) Heat maps corresponding to single-cell analysis of data in part a after *k*-means clustering, where the response of each individual cell is represented in each row for the duration of the experiment. Colormap is normalized to the data of highest concentration for each frequency.

μM. Above 3.75 μM cells responded with a higher $[Ca^{2+}]i$ increase but the size of the response decreased for the subsequent agonist applications. A similar phenomenon of response size falling-off has been reported by others.[29] However, the percentage of responding cells at 20 mHz remained almost flat from the lowest concentration on, and it only increased slightly to ∼30% at the highest agonist concentration used (10 μM). We noticed responses of a minority of cells when stimulated with PBS at 20 mHz. This phenomenon has been reported in conditions where the fluid flow is changed abruptly (stop-flow method), such as in our case.[30] Membrane deformation can activate mechanoreceptive ion channels that induce Ca^{2+} entry of into the cytoplasm.[30] This infrequent artifact does not invalidate the results obtained with carbachol. In conclusion, these experiments demonstrate the utility of our device to generate chemical stimuli of different frequencies and agonist concentration, which allows us to analyze the release of Ca^{2+} from intracellular stores of ∼2200 individual cells under different stimulation parameters. Our results indicate that HEK-293 cells constitute a heterogeneous population judging by the cell-to-cell response differences to the same stimulus. This is in spite of the fact that at increasing agonist concentrations, the percentage of responsive cells increases linearly with concentration regardless of the rate of stimulation. In addition, results obtained with our microfluidic platform could also contribute to the development of more realistic mathematical models of Ca^{2+} signaling.[31]

CONCLUSIONS

We have described the design and operation of an integrated microfluidic device engineered to generate chemical waveforms of different amplitude with the same frequency. The resulting concentrations are delivered to a set of nine chambers, each containing an array of 492 microwells for capturing individual cells. The response of each cell to a dynamic input can be measured while it is maintained under a low shear stress perfusion over the microwell. The frequency of the stimulus can be adjusted from a computer to a maximum operating frequency of 33.3 mHz. This operating frequency is a drawback of our device which would limit its use in cellular process faster than 15 s. It is possible to scale down the microchambers to include less microwells and thus increase this frequency but at the expense of interrogating less cells.

Importantly, our design is modular, and the linear gradient generator described here can be easily replaced by other types of gradient generators. In combination with the microwells, the device can be used to study single cells responses under time-varying stimuli. For example, our device could be used to study the dynamics of transcription factors translocation to the nucleus to control gene expression in mammalian cells, such as NF-κB. Another potential application is the study of the dynamics of proteins in single cells under different drug conditions.[32] Also interesting is the identification and study of cell subtypes in a mixed population (i.e., blood cells), without the time-consuming and potentially detrimental cell separation procedures, although this would require a redesign of the microchambers to contain a large number of microwells. By focusing on the subset of responding cells, dose response curves to a given agonist or drug can be constructed.

Although we described the device characterization and performance to the study $[Ca^{2+}]i$ dynamics of HEK cells, it can be easily adopted to study the dynamics of any other type of intracellular messenger or cell type. Our microfluidic device could be used as a high-throughput platform to perform many types of pharmacological or biological assays with single-cell resolution, as long as the desired cellular mechanism relies on a fluorescence signal for its analysis.

ASSOCIATED CONTENT

Supporting Information

The Supporting Information is available free of charge on the ACS Publications website at DOI: 10.1021/acs.analchem.8b02442.

Detailed fabrication of the microfluidic device, list of reagents, comparison between our device and previously reported devices to analyze single cells under different conditions, microfluidic device design, simulation of 2D shear-stress on cells positioned at different heights inside microwells, maximum shear stress at different inlet flow rates on cells located at different heights in the microwells, characterization of the concentration gradient generator (CGG), normalized concentration gradient profiles generated in each chamber at different flow rates, characterization of the time required to exchange a solution in sections of a microchamber, single-cell analysis using Matlab, graph of the mean fluorescence intensity over time measured in each of the nine chambers for Calcein-AM staining, single-cell Calcein-AM response at each chamber, Gaussian fit parameters for histograms in Figure S7, single-cell

DOI: 10.1021/acs.analchem.8b02442
Anal. Chem. XXXX, XXX, XXX−XXX

responses to carbachol stimulation at 4.5 mHz, periodic stimulation of HEK-293 cells with carbachol at 20 mHz, and single-cell responses to carbachol stimulation at 20 mHz (PDF)

Video of one chamber where fluid is alternated between D-R and PBS at a frequency of 7.4 mHz (MPG)

Video showing cells stained with Fluo-8-AM being stimulated with a pulse of 10 s of carbachol (MPG)

AUTHOR INFORMATION

Corresponding Author

*E-mail: jlgarciac@cinvestav.mx.

ORCID

Jose L. Garcia-Cordero: 0000-0002-3868-7405

Author Contributions

The manuscript was written through contributions of all authors.

Notes

The authors declare no competing financial interest.

ACKNOWLEDGMENTS

We would like to thank Rocio Jimenez-Valdes and Arturo Picones for fruitful discussions, D. Millán-Aldaco and C. Lara-Figueroa for tissue culture, and J. C. Gomora for HEK 293 cells. This work was funded by Mexico's CONACyT Grants CB-256097, AEM-262771, and FC-1132 (to J.L.G.-C.) and Grants CB-240305, 279820 (LaNCa) (to A.H.-C.). We also thank support from CIC UNAM/Dr. William Lee and Grant PAPIIT- IN211616.

REFERENCES

(1) Purvis, J. E.; Lahav, G. *Cell* **2013**, *152* (5), 945−956.

(2) Behar, M.; Hoffmann, A. *Curr. Opin. Genet. Dev.* **2010**, *20* (6), 684−693.

(3) Brent, R. *FEBS Lett.* **2009**, *583* (24), 4019−4024.

(4) Chingozha, L.; Zhan, M.; Zhu, C.; Lu, H. *Anal. Chem.* **2014**, *86* (20), 10138−10147.

(5) Sumit, M.; Takayama, S.; Linderman, J. *Integr. Biol.* **2017**, *9* (1), 6−21.

(6) Hlavacek, W. S.; Faeder, J. R. *Sci. Signaling* **2009**, *2* (81), pe46.

(7) Loewer, A.; Lahav, G. *Curr. Opin. Genet. Dev.* **2011**, *21* (6), 753−758.

(8) He, L.; Kniss, A.; San-Miguel, A.; Rouse, T.; Kemp, M. L.; Lu, H. *Lab Chip* **2015**, *15* (6), 1497−1507.

(9) Huang, P.-H.; Chan, C. Y.; Li, P.; Wang, Y.; Nama, N.; Bachman, H.; Huang, T. J. *Lab Chip* **2018**, *18*, 1411−1421.

(10) Olofsson, J.; Bridle, H.; Sinclair, J.; Granfeldt, D.; Sahlin, E.; Orwar, O. *Proc. Natl. Acad. Sci. U. S. A.* **2005**, *102* (23), 8097−8102.

(11) Chen, L.; Azizi, F.; Mastrangelo, C. H. *Lab Chip* **2007**, *7* (7), 850.

(12) Chen, P.; Guo, Y.; Feng, X.; Yan, S.; Wang, J.; Li, Y.; Du, W.; Liu, B. F. *Anal. Chem.* **2017**, *89* (17), 9209−9217.

(13) Ainla, A.; Gözen, I.; Orwar, O.; Jesorka, A. *Anal. Chem.* **2009**, *81* (13), 5549−5556.

(14) Woodruff, K.; Maerkl, S. J. *Anal. Chem.* **2018**, *90* (1), 696−701.

(15) Zhang, X.; Grimley, A.; Bertram, R.; Roper, M. G. *Anal. Chem.* **2010**, *82* (15), 6704−6711.

(16) Piehler, A.; Ghorashian, N.; Zhang, C.; Tay, S. *Lab Chip* **2017**, *17* (13), 2218−2224.

(17) Kniss-James, A. S.; Rivet, C. A.; Chingozha, L.; Lu, H.; Kemp, M. L. *Integr. Biol.* **2017**, *9* (3), 238−247.

(18) Chen, P.; Feng, X.; Yan, S.; Guo, Y.; Wang, J.; Li, Y.; Chen, D.; Du, W.; Liu, B.-F. *Sens. Actuators, B* **2018**, *263*, 281−288.

(19) Pelkmans, L. *Science* **2012**, *336* (6080), 425−426.

(20) Stepanenko, A. A.; Dmitrenko, V. V. *Gene* **2015**, *569* (2), 182−190.

(21) Campbell, K.; Groisman, A. *Lab Chip* **2007**, *7*, 264−272.

(22) Jimenez-Valdes, R. J.; Rodriguez-Moncayo, R.; Cedillo-Alcantar, D. F.; Garcia-Cordero, J. L. *Anal. Chem.* **2017**, *89* (10), 5210−5220.

(23) Nakamura, N.; Yamazawa, T.; Okubo, Y.; Iino, M. *Mol. Syst. Biol.* **2009**, *5* (247), 247.

(24) Berridge, M. J.; Bootman, M. D.; Roderick, H. L. *Nat. Rev. Mol. Cell Biol.* **2003**, *4* (7), 517−529.

(25) Verkhratsky, A. In *Calcium Signalling and Disease*; Springer Netherlands: Dordrecht, The Netherlands, 2007; pp 465−480.

(26) Hussmann, G. P.; Yasuda, R. P.; Xiao, Y.; Wolfe, B. B.; Kellar, K. J. *J. Biol. Chem.* **2011**, *286* (46), 39726−39737.

(27) Giorgi, C.; Danese, A.; Missiroli, S.; Patergnani, S.; Pinton, P. *Trends Cell Biol.* **2018**, *28* (4), 258−273.

(28) Dupont, G.; Combettes, L.; Leybaert, L. *Int. Rev. Cytol.* **2007**, *261*, 193−245.

(29) Jovic, A.; Wade, S. M.; Miyawaki, A.; Neubig, R. R.; Linderman, J. J.; Takayama, S. *Mol. BioSyst.* **2011**, *7* (7), 2238.

(30) Tong, J.; Du, G. G.; Chen, S. R. W.; MacLennan, D. H. *Biochem. J.* **1999**, *343* (1), 39−44.

(31) Jovic, A.; Wade, S. M.; Neubig, R. R.; Linderman, J. J.; Takayama, S. *Integr. Biol.* **2013**, *5* (7), 932.

(32) Cohen, A. A.; Geva-Zatorsky, N.; Eden, E.; Frenkel-Morgenstern, M.; Issaeva, I.; Sigal, A.; Milo, R.; Cohen-Saidon, C.; Liron, Y.; Kam, Z.; et al. *Science* **2008**, *322* (5907), 1511−1516.

DOI: 10.1021/acs.analchem.8b02442
Anal. Chem. XXXX, XXX, XXX−XXX